6.1. Materials

Table 6.1: List of the chemicals and reagents used during the study

S. No.	Materials	Suppliers
1.	Ciprofloxacin	Cadila Healthcare Ltd. Ahmadabad (India)
2.	Chitosan (140KD Mo. Wt.; ≥75% Deacetylated	Sigma-Aldrich, Banglore (India)
3.	Alginate lyase	Sigma-Aldrich, Banglore (India)
4.	Live/Dead cell viability kit (SYTO9/Propidium iodide)	Thermo Fischer Scientific, India
5.	Sodium Tri-polyphosphate (TPP)	
4	Potassium Dihydrogen Orthophosphate	Qualigens Fine Chemicals, Mumbai.
5	Di-Sodium Hydrogen Orthophosphate Anhydrous	Qualigens Fine Chemicals, Mumbai.
6	Polyethylene Glycol 600	Merck Limited, Mumbai
7	Acetic Acid For Hplc And Spectroscopy	S D Fine-Chem Limited, Mumbai.
8	Diethyl Ether Ar	S D Fine-Chem Limited, Mumbai.
9	Silver Sulfadiazine Cream Usp 1% W/W	Hind Pharma, Bhopal.
10	O-Phosphoric Acid	Spectrochem Pvt Ltd, Mumbai
11	Sorbitane Monooleate Lr	S D Fine-Chem Limited, Mumbai.
14	Type 1 Water	Arium® Pro Ultrapure Water Systems

6.2. Methods

6.2.1. Analytical Method

6.2.1.1. Ciprofloxacin Stock Solution

Accurately weighed 50 mg of ciprofloxacin was dissolved in the 100 mL distilled water to produce the stock solution of 500 µg/mL concentration. To obtain the calibration

curve of ciprofloxacin in the water and phosphate buffer saline (PBS) pH 6.8, the stock solution was appropriately diluted using the respective solution.

6.2.1.2. UV spectrophotometric calibration curve in water

Initially, the stock solution of ciprofloxacin was diluted properly using the distilled water to obtain the concentration 2, 4, 6, 8 and 10 µg/mL. Subsequently, the dilutions were scanned over the UV range from 200 – 400 nm to determine the absorbance maxima (λ_{max}). Finally, absorbance values corresponding to all the dilutions were determined at λ_{max} (279 nm) and used to prepare the calibration curve.

6.2.1.3. UV spectrophotometric calibration curve in PBS pH 6.8

Initially, the stock solution of ciprofloxacin was diluted properly using the PBS pH 6.8 to obtain the concentration 2, 4, 6, 8 and 10 µg/mL. Subsequently, the dilutions were scanned over the UV range from 200 – 400 nm to determine the absorbance maxima (λ_{max}). Finally, absorbance values corresponding to all the dilutions were determined at λ_{max} (279 nm) and used to prepare the calibration curve.

6.2.2. Fabrication of chitosan nanoparticles

Ciprofloxacin loaded chitosan nanoparticles (CIPR-CH-NPs) were prepared by ionotropic gelation technique with Tri-poly phosphate (TPP) as a polyanionic crosslinking agent (Grenha, Seijo et al. 2007, Al-Qadi, Grenha et al. 2012, Harde, Agrawal et al. 2014). Concisely, the chitosan was added in acetic acid (0.1% v/v; pH 3.5) and allowed overnight with continuous stirring to obtain the 0.1% w/v clear solution of chitosan. In the next step, ciprofloxacin in the ratio 1:5 was dissolved in it. Further, pH was adjusted to 6.0-6.5 with 1N NaOH followed by drop wise addition of cross-linking agent (0.1% w/v TPP in water) in 1:4 ratio to the chitosan solution with continuous stirring (1200 rpm) on magnetic stirrer at room temperature.

Finally, the carbodiimide chemistry was employed to form the AgLase functionalized chitosan nanoparticles of ciprofloxacin (AgLase-CIPR-CH-NPs) (Hou, Yu et al. 2017). Initially, 100 µg/mL of AgLase was mixed with 0.1M EDAC, and 0.1 M NHS solution to form the activated ester of AgLase and the activation was followed by 30 min reaction of the cross-linked chitosan nanoparticles with activated AgLase to form the amide bond between the free amine groups of the chitosan to the carboxyl group of AgLase at room temperature with continuous stirring. Further, the reaction mixture was centrifuged on 10 µL glycerol bed in centrifuge tube (1600xg for 20 minutes) to remove the soluble reagents and byproduct.

6.2.3. Preparation of inhalable powder

Enzymes (AgLase) being the temperature sensitive, freeze drying was employed to prepare the inhalable powder of nanoparticles using lactose as cryoprotectant. Precisely, the three step process comprised of pre-freezing of nanoparticles for 1h at -40^{o}C followed by primary drying at -20^{o}C for 24h to sublimate the ice. Immediately after primary drying, secondary dying at 20^{o}C for 24h maintained at 1Pa pressure to remove the elimination of absorbed water not sublimate off. Eventually, the AgLase-CIPR-CH-NPs were allowed to be adsorbed on the micronized dry lactose powder (InhaLac-500, Meggle) to achieve the uniform particles appropriate for inhalation and improve the stability without disturbing the peculiarity of NPs. Briefly, the freeze dried NPs were blended with micronized dry lactose powder at controlled relative humidity (50±5%) in the ratio 95:05. Subsequently, angle of repose of prepared powder was measured to determine the flow property.

6.2.4. In-vitro aerodynamic properties of dry powder

Mass median aerodynamic diameter (MMAD) of prepared freeze dried AgLase-CIPR-CH-NPs adsorbed inhalable lactose powder was determined by 8 stage Anderson cascade impactor (ACI) with effective cut off diameter 9 (Stage 0), 5.8 (stage 1), 4.7 (stage 2), 3.3 (stage 3), 2.1 (stage 4), 1.1 (stage 5), 0.65 (stage 6) and 0.43 µm (stage 7) (Yang, Bajaj et al. 2009). Precisely, 200 mg powder was loaded in the size 3 gelatin capsule and placed in Rotahaler for release of powders from induction port in ACI with a flow of 28.3 L/min for 10 min. The glass filters used to prevent the re-entrainment of particles were weighed to determine the exact amount of particles deposited by weight difference. Further, fine particle fraction (FPF) and MMAD was calculated from the amount deposited at different stages. The particles below the cut of diameter 4.7 µm (collected below stage 2) are generally considered as the fine-particles and the ratio of fine particles weight to the initial dose of powder filled in the Rotahaler is termed as fine particle fraction (FPF). The MMAD and FPF are essential parameter to predict the extent of particles deposition in the lungs. Interestingly, major portion of fine particle fraction considered to be deposited in the lower respiratory region while the majority of particles with 4.7 µm and above size deposits in the upper respiratory tract.

6.2.5. Identification of AgLase Conjugation

A modified Ninhydrin method for quantification of amino group in chitosan was used to confirm the conjugation (Prochazkova, Vårum et al. 1999). The absorbance at 570 nm for cross linked CIPR-CH-NPs and AgLase-CIPR-CH-NPs (50 µg/mL) was measured and compared with absorbance of Mixture. The percentage of free amino group was determined using the following formula:

$$\% \textbf{ free Amino Group} = \frac{\boldsymbol{A570\ AgLase - CIPR - CH - NPs}}{\boldsymbol{A570\ for\ Chitosan\ in\ CIPR - CH - NPs}}\ \boldsymbol{x}\ \mathbf{100}$$

Here, A570 represents the absorbance of Chitosan and AgLase in each sample.

6.2.6. Enzyme activity assay of AgLase bearing NPs

Enzyme activity was performed as per the method reported in the previous study (Chen, Zhu et al. 2018). The assay was performed in 96 well plates with five replicates for each group. Briefly, 200 µL of Sodium alginate solution (10 mg/mL) in phosphate buffer (pH 6.5) was incubated with 50 µL AgLase (20 µg/mL) for 30 min at 37°C. Finally, 20 µL of 10M NaOH was added to stop the reaction and absorbance at 235 nm was recorded using microplate reader (SYNERGY/HTX, Biotek). Here, one unit (U) enzyme is the amount that increases the absorbance by 1/min at 235 nm. The activity was represented at % activity with reference to the pure AgLase.

6.2.7. Particle Size (PS), polydispersity index (PDI) and zeta potential (ZP) analysis

PS, PDI, and ZP were analyzed using DelsaNanoC (Beckman coulter, USA). Nanoparticles suspension was diluted ten times before analysis and placed in the respective cell for analysis. PS and PDI were the average of three measurement cycle of 50 seconds based on differential light scattering principle, whereas values of ZP was determined based on the electrophoretic movement of the charged particle in the applied electric field in mV.

6.2.8. Entrapment efficiency (EE)

Entrapment efficiency was calculated by UV spectrophotometric method (Shimadzu 1800, Tokyo, Japan) at 279 nm. The upper chamber of nanosep tube was filled with 500 µL of nanosuspension and centrifuged at 15000 rpm for 10 min (10°C). The filtrate

diluted appropriately and absorbance was recorded at 279 nm. Finally, the free drug concentration was determined using the calibration curve to calculate the % EE of the suspension by the following formula;

$$\% \mathbf{EE} = \frac{\mathbf{Total\ drug\ added\ initially - Free\ drug\ in\ suspension}}{\boldsymbol{Total\ Drug\ added\ initially}} \boldsymbol{X}\ \mathbf{100}$$

6.2.9. Scanning electron microscopy (SEM)

Shape and surface morphology of optimized CIPR-CH-NPs and AgLase-CIPR-CH-NPs were investigated by SEM (ZEISS, EVO18, Germany). The sample was prepared by drying the single drop on copper foil. Subsequently, the dried layer was coated with gold and observed under SEM to obtain the image.

6.2.10. *In-vitro* release

In-vitro release study was carried using dialysis bag technique in phosphate buffer saline (PBS) pH 6.8. Briefly, sample equivalent to 2 mg of ciprofloxacin was kept in the cellulose dialysis membrane bag (molecular weight cut off 12kDa, HiMedia Laboratories), and immersed in the beaker containing 100 mL Phosphate buffer saline (PBS). Disodium hydrogen phosphate (2.38 gm), potassium dihydrogen phosphate (0.19 gm), and NaCl (8.0 gm) in 1000 mL were the main component in the PBS. The system was maintained at 37°C with continuous stirring (50 rpm) on hot plate magnetic stirrer (IKA, Germany). Samples (1 mL) were withdrawn at the definite time points and replaced with fresh PBS. Finally, UV absorbance was recorded at 279 nm after proper dilution. The release data was plotted for different kinetic equation including first order, zero order, Higuchi equation and Korsmeyer-Peppas to find out the release mechanism and kinetics.

6.2.11. Fourier transform infrared spectroscopy (FT-IR)

FTIR spectroscopy was performed to assess the possible interaction between drug and excipients using IR spectrophotometer (SHIMADZU; 8400S, Japan). The KBr disc method was used to derive the spectra. Samples were scanned over the range of 400-4000 cm^{-1} wave number with the resolution of 2 cm^{-1}. Finally, the spectra were obtained and analyzed.

6.2.12. X-ray diffraction (XRD)

XRD spectra were derived with diffraction angle 2θ ranging from 10-80° using X-ray diffractometer (Rigaku, MiniFlex 600, Japan). Powdered sample was dispersed on the quartz sample holder and placed on goniometer to record the diffraction pattern at all possible angle of diffraction using detector DTEX at the scanning rate of 5°/min. Spectra were collected and analyzed.

6.2.13. Collection of mucoid *P. aeruginosa*, characterization and culture growth

Mucoid *P. aeruginosa* was collected from the clinical sample coming to Department of microbiology, Institute of Medical Sciences, Banaras Hindu University, Varanasi, India. The isolated strain was identified using routine biochemical testing such as oxidative fermentative test, sulfur indole motility test, lactose, glucose, sucrose, urease and simmon citrate test (Saxena, Banerjee et al. 2014). The isolated strain of mucoid *P. aeruginosa* was further identified by Muir mordant staining which gives rise to red color (Owlia, Nosrati et al. 2014). The identified strain was plated in Luria Bertani (LB) (Pronadisa, Spain) medium at 37°C to grow overnight. After overnight growth, the absorbance of the centrifuged sample (at 5000 rpm for 10 min) was recorded at λ_{max} 550 nm to confirm the bacterial cell growth.

6.2.14. Minimum inhibitory concentration (MIC)

Two-fold broth dilution method was employed to find the MIC of ciprofloxacin and nanoparticle formulations against *P. aeruginosa.* Bacterial culture (100 µL, $0.5x10^6$ CFU/mL) was seeded in the 96 well culture plate (Polystyrene, transparent, sterile, BRAND plates) and incubated at 37°C for 48 h with 100 µL of different samples including free ciprofloxacin and nanoparticles with concentration of ciprofloxacin ranging from 4, 2, 1, 0.5, 0.25, 0.125, 0.0625, 0.0312, and 0.0156 µg/mL. Additionally, we also performed the MIC study for Chitosan, CH-NPs, AgLase-CH-NPs without CIPR (Concentration varied from 10, 5, 2.5, 1.25, 0.625, 0.312, 0.156, 0.078, and 0.039 mg/mL) and Aglase (concentration ranging from 100, 50, 25, 12.5, 6.12, 3.06, 1.53, 0.76, 0.38 and 0.0156 µg/mL). Finally, the absorbance values of incubated samples were recorded on the multi-mode plate reader (SYNERGY/HTX, Biotek) at 550 nm at 24 and 48 h.

6.2.15. Minimum biofilm inhibitory concentration (MBIC)

MBIC of different formulation samples was determined on peg lids of 96 well plate (Baelo, Levato et al. 2015). Precisely, 100 µL of *P. aeruginosa* (0.5×10^5 CFU/mL) suspension in LB medium was plated in the 96 well plate and then different test samples were instilled to the specified row (at 1, 0.5, 0.25, 0.125, 0.0625, 0.0312, and 0.0156 µg/mL concentration). The plates were incubated at 37°C for 48 h on the rotary shaker. Eventually, loosely adhered planktonic bacteria on peg lids were washed thrice by PBS and biofilm producing cell was recovered in 200 µL LB using ultrasonication for 5 min. Recovered cells were serially diluted and plated on LB agar plates, and colony-forming units were counted after 24 and 48 h.

6.2.16. Minimum biofilm eradication concentration (MBEC)

MBEC for different samples was evaluated using the biofilm grown on the peg lid (Olson, Ceri et al. 2002). Briefly, 96 well culture plate (Polystyrene, transparent, sterile, BRAND plates) filled with 200 µL, $0.5x10^6$ CFU/mL of *P. aeruginosa* bacterial culture in LB medium was covered with peg lid and incubated at 37°C for 48 h on the rotary shaker to form the biofilm on peg. Methylene blue dye test confirmed the production of biofilm. After 48 h, peg lid holding the biofilm was washed thrice with PBS to remove the adhered planktonic bacteria and then the biofilm containing peg lid was covered over the 96 well plate containing different test samples. The concentration of different samples varied from 4, 2, 1, 0.5, 0.25, 0.125, 0.0625, 0.0312 and 0.0156 µg/mL diluted in the LB medium. In addition, biofilm eradication property of Chitosan, CH-NPs, and AgLase-CH-NPs without CIPR (Concentration varied from 10, 5, 2.5, 1.25, 0.625, 0.312, 0.156, 0.078, and 0.039 mg/mL) was also determined. The system was incubated for 24 h at 37°C. After 24 h, peg lids were removed and placed on the second 96 well plate containing fresh LB medium for sonication to remove the adhere biofilm. Recovered cells were serially diluted and plated on LB agar plates, to count the CFU. Additionally, the biofilm was treated with repeated dose (0.125 µg/mL) for three days to evaluate the biofilm eradication potential at MIC of NPs

6.2.17. Biofilm formation on coverslip and microscopy

Biofilm was grown on the 12 mm diameter coverslip in 12 well plate according to the previous study (Mu, Tang et al. 2016). Briefly, coverslip containing biofilm was removed from the plate after 48 h and washed gently using PBS to remove the loosely adhered bacterial cell. Further, the coverslip was transferred to the second 12 well plate for the treatment with different testing samples (0.125 µg/mL) in LB. After 24 h of treatment, the coverslip was removed, and the cells were fixed using 4% w/v

paraformaldehyde. Eventually, biofilm was stained with LIVE/DEAD BacLight Bacterial Viability kit (Thermo Fischer, India) in the dark according to manual (6 μM SYTO 9 and 30 μM propidium iodide) at room temperature.

Confocal laser scanning microscopic (CLSM) images of biofilm were acquired using ZEISS, Germany. Sections were scanned at the excitation wavelength of 488, and 560 nm with 40X magnification and Z-stack were obtained at z step size of 2.03 μm. Finally, the acquired images were processed using COMSTAT-2 to get the thickness and biomass of biofilm in case of different treatments.

6.2.18. MTT assay

Cell toxicity was evaluated by 3-[4,5-dimethylthiazol-2-yl]-2,5-diphenyltetrazolium bromide (MTT) test. MTT assay is principally based on the formation of colored formazan precipitate in the mixture. In this study, 2.0×10^4 lung epithelium cells (BEAS-2B, ATCC) seeded in 96 well plate were incubated with increasing concentration of CIPR-CH-NPs or left untreated as control. At the end of 24 h of incubation of cells with varying concentrations of the NPs, 10% MTT prepared in the medium was instilled into each well after removing the culture supernatant and incubated for the defined time. A blue colored, water-insoluble formazan precipitates obtained after MTT treatment were dissolved in the DMSO and the absorbance at 550 nm was recorded.

6.2.19. Haemocompatibility studies

6.2.19.1. Haemolysis Study

Haemolysis study was performed on human blood purchased from authorized blood bank as per the protocol followed in the previous study (Vijayakumar, Kumari et al. 2016). The equal volume normal saline was mixed gently to the plasma free blood

sample obtained after centrifugation of 2 mL blood at 500 rpm for 10 min at room temperature in a sterile graduated centrifuge tube. Further, the blood sample was centrifuged and washed thrice using the normal saline following the same protocol. Eventually, the erythrocytes were suspended in the normal saline and made the volume up to 10 mL. CIPR, CIPR-CH-NPs and AgLase-CIPR-CH-NPs (equivalent to 0.0625, 0.125 and 0.25 µg/mL of CIPR), and AgLase (equivalent to 10, 50 and 100 µg/mL were incubated with 2 mL of erythrocyte suspension in Eppendorf tubes for 8 h at 37°C. The blood sample treated with 1% triton 100X (100% haemolysis) and normal saline were taken as positive control and negative controls, respectively. The entire samples were gently shaken after every 30 min. After 8 h the sample were centrifuged at 5000 rpm for 10 min and the obtained supernatant were incubated at room temperature for 30 min to allow the oxidation to haemoglobin. Finally, the % haemolysis was calculated from the absorbance measured spectrophotometrically at 540 nm by the following equation;

$$\% \textbf{ haemolysis} = \frac{\boldsymbol{A}(\textbf{Test sample}) - \boldsymbol{A}\ (\boldsymbol{negative\ control})}{\boldsymbol{A}(\boldsymbol{positive\ control})}\ \boldsymbol{X}\ \textbf{100}$$

6.2.19.2. Platelet aggregation

Platelet aggregation was determined by using haematological counter (Multisizer 4, Beckmann Coulter, USA) as per the previous reports (Vijayakumar, Kumari et al. 2016). Whole blood sample (1 mL) was incubated with CIPR, CIPR-CH-NPs and AgLase-CIPR-CH-NPs (0.0625, 0.125 and 0.25 µg/mL of CIPR) and AgLase (10, 50, 100 µg/mL) at 37°C for 2 h. Also, blood sample treated with PBS (pH 7.4) was taken as control. Subsequently the diluted samples were examined using haematological counter (Multisizer 4, Beckmann Coulter, USA).

Furthermore, the treated blood samples were stained using Leishman's stain (Span Diagnostics, India) for 5 min on prepared peripheral smears for qualitative analysis of platelet aggregation. The images of stained smears were captured by digital camera with an optical microscope.

6.2.20. *In-vivo* toxicity study

In this study, male Wistar rats, weighing 200–250 gm procured from animal house, Institute of Medical Sciences, Banaras Hindu University, Varanasi were divided into 5 treatment groups (n=3) *viz.* untreated control, CIPR, AgLase, CIPR-CH-NPs and AgLAse-CIPR-CH-NPs. The Central Animal Ethical Committee, Faculty of Medicine, Institute of Medical Sciences, Banaras Hindu University approved the given protocol for lung toxicity study.

The in-house inhalation apparatus was used to administer the powdered formulations by pulmonary route as per the procedure described by Muttil et al., 2007 (Muttil, Kaur et al. 2007). Test samples (10 mg) were placed on the cap of 15 mL centrifuged tube and fluidized by introducing turbulent air through the hole at the apex of tube with the help of actuating rubber pipette bulb. At the same time the nares of rats were inserted in the hole at the wall of tube to inhale the fluidized formulation for 30 sec. The procedure was repeated for 7 consecutive days and then the animals were sacrificed to remove the formulation exposed lungs. Finally, the transverse section of lung tissue was prepared using the Cryostat (Leica, Germany) to prepare the glass smears. The prepared smears were stained using Haemotoxylin and Eosin (HE) and after proper washing the HE stained smears were observed under light microscope to capture the images of tissue. The images were observed and evaluated for the evidence of toxicity, if any.

6.2.21. Statistical analysis

The data was statistically analyzed using software GraphPad Prism 5.0 (GraphPad Software Inc., San Diego, CA).

6.3. Results and Discussion

6.3.1. Analytical method

The calibration curve was prepared to extrapolate the ciprofloxacin concentration in in-vitro release samples and also to determination of the entrapment efficiency of CIPR in the nanoparticles. The UV calibration curve of the ciprofloxacin was successfully prepared in water and phosphate buffer pH 6.8 with higher linearity 0.9996 and 0.9994 (Figure 6.1 and 6.2), respectively.

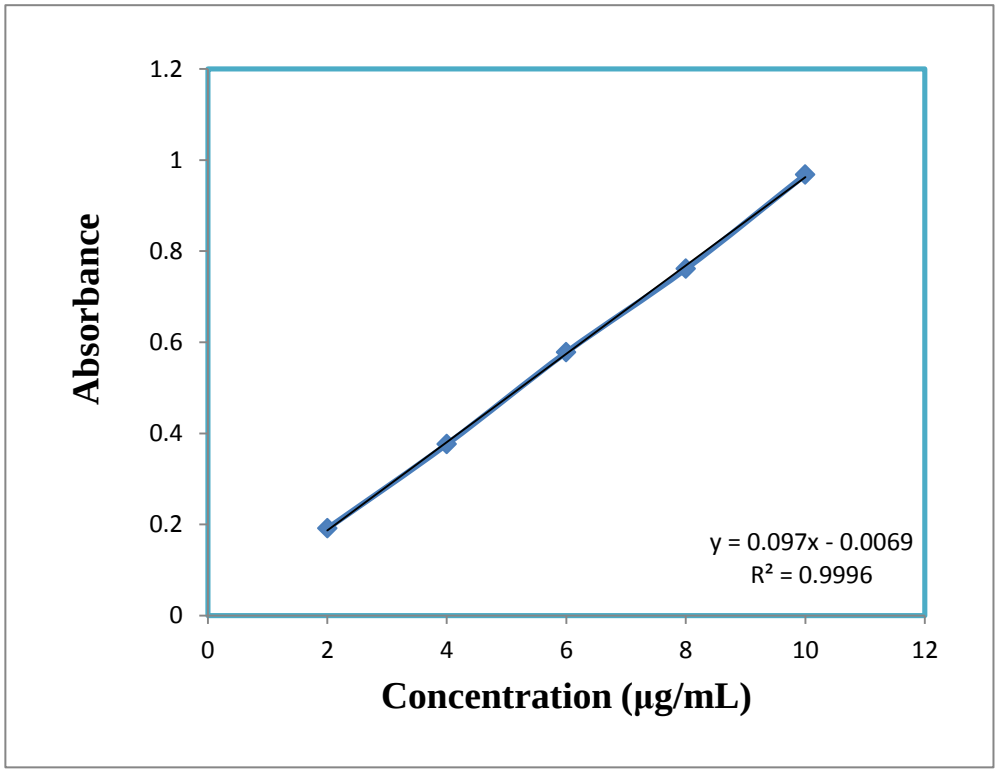

Figure 6.1: UV Spectrophotomtric calibration curve of ciprofloxacin in water

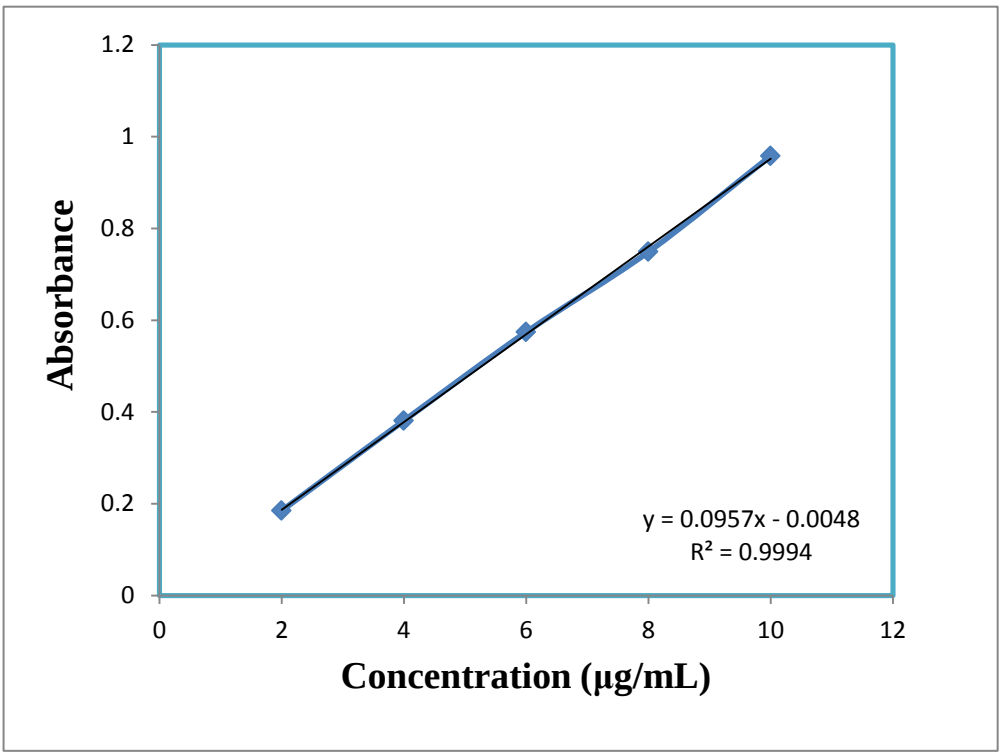

Figure 6.2: UV Spectrophotomtric calibration curve of ciprofloxacin in water**.**

6.3.2. AgLase conjugation and enzyme assay

The findings of the conjugation study were calculated as free amino group in each formulation, keeping the CIPR-CH-NPs with 100% free amino groups (shown in Figure 6.3). AgLase-CIPR-CH-NPs exhibited 44.2±5.3% free amino group. The data suggested that approximately 55.8% amino groups of chitosan conjugated with the AgLase during functionalization. Meanwhile, the results of enzyme assay for AgLase-CIPR-CH-NPs shown in figure 6.4 demonstrated around 61.2±4.3% activity compared to pure AgLase, whereas, the CIPR-CH-NPs+AgLase imparted almost similar activity profile with pure enzyme.

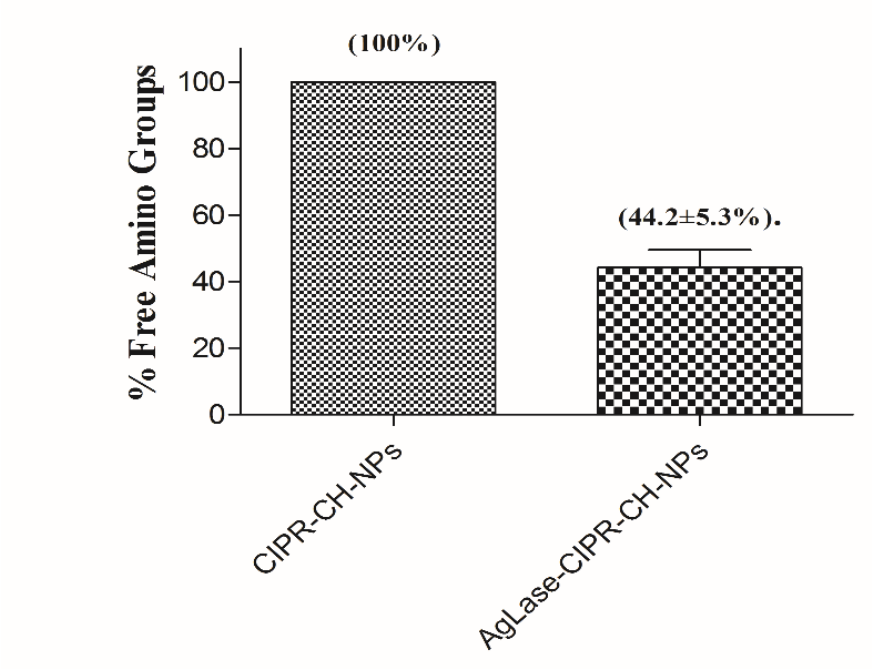

Figure 6.3: Percentage free amino groups remained after conjugation in AgLase-CIPR-Ch-NPs.

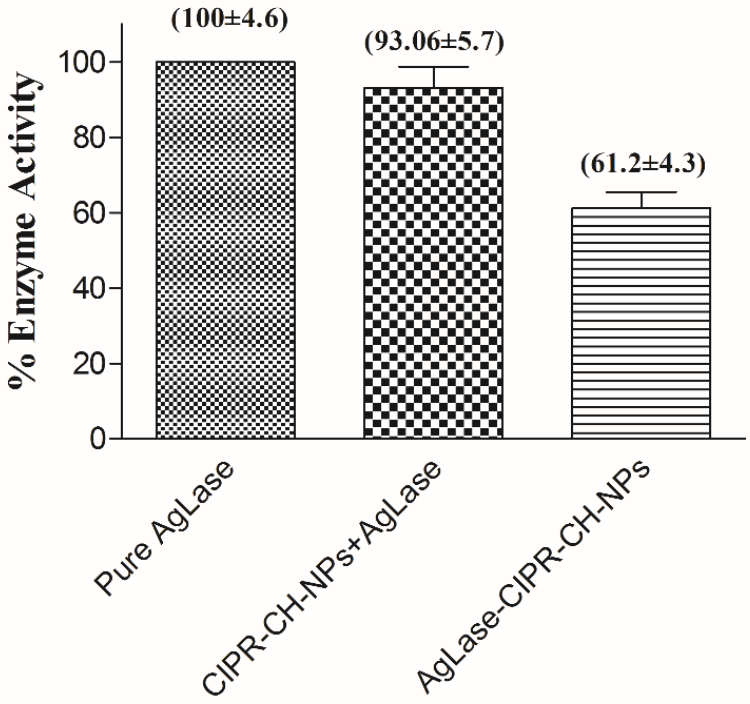

Figure 6.4: Percent hydrolytic activity of the AgLase-CIPR-CH-NPs after conjugation as compared to pure AgLase.

6.3.3. Particle characterization (PS, PDI, ZP, and EE)

CIPR-CH-NPs were prepared using the ionotropic gelation method to achieve the desired particle characteristics. Further, EDC and NHS were used to functionalize the CIPR-CH-NPs with AgLase by presenting the activated ester of alginate lyase to the amino group on chitosan (Hou, Yu et al. 2017). The quality attributes in terms of PS, PDI, ZP, and EE of different nanoformulations are given in Table 6.2. The AgLase-CIPR-CH-NPs had 205.5±9.0 nm PS, 0.302±0.031 PDI, 12.2±2.1 mV ZP and 51.8±2.1 %EE, respectively. The PS was increased slightly perhaps due to immobilization of AgLase molecule on NPs surface. Interestingly, AgLase-CIPR-CH-NPs with such particle diameter can readily diffuse through thick mucus pores in infected lungs in cystic fibrosis (Suk, Lai et al. 2009) and can effectively deliver the drug nearby of microbial colonies. The value of zeta potential decreased slightly from 14.6±1.2 to 12.2±2.1 mV following the functionalization. Moreover, the EE efficiency obtained was lower as expected and could be assigned to the hydrophilic nature of the drug (Bilati, Allémann et al. 2005). However, EE was unaffected with surface modification of chitosan NPs.

Table 6.2: Quality attributes of different formulations in terms of Particle size, polydispersity index, zeta potential and entrapment efficiency.

S. no.	**Formulation**	**Characterization**			
		PS* (nm)	**PDI***	**ZP* (mV)**	**EE* (%)**
1.	CIPR-CH-NPs	191.1±8.9	0.257±0.042	14.6±1.2	54.9±3.6
2.	AgLase-CIPR -CH-NPs	205.5±9.0	0.302±0.031	12.2±2.1	51.8±2.1

*****value represents mean of 3 replicates with standard deviation (Mean±SD)

6.3.4. SEM analysis

SEM analysis was performed to evaluate the surface morphology and also to determine the particle size of the nanoparticles. Surface morphology (shape and size) depicted in Figure 6.5 & 6.6 of NPs showed that particles had the spherical shape, and equivalent or somewhat smaller PS than measured by DLS and could be explained by obvious difference between the hydrodynamic diameter (measured by DLS) and the actual diameter (measured by SEM).

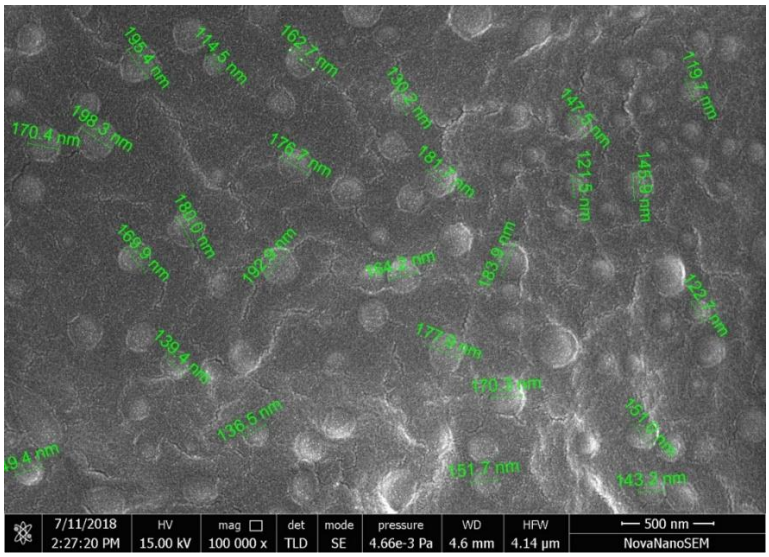

Figure 6.5: SEM micrograph of the CIPR-CH-NPs.

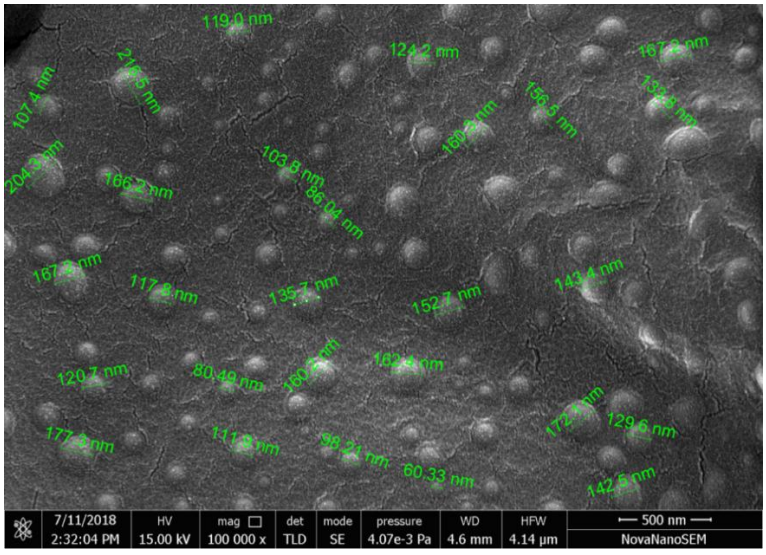

Figure 6.6: SEM micrograph of AgLase-CIPR-CH-NPs.

6.3.5. Characterization of Freeze dried powder

The Angle of repose of freeze dried inhalable NPs was determined to make sure the free flow of powder during inhalation from devise. However, higher value for FPF and MMAD >1 µm ensure the higher lung deposition and effective lung targeting of proposed NPs adsorbed on lactose. Further, the Lactose adsorbed NPs demonstrated fair particle flow with angle of repose, 33.4^{o} and aerodynamic MMAD, 2.69±0.03 µm and FPF, 38±2.7% sufficient enough to achieve significant lung deposition of nanoparticle and stability thereof. The good flow property help in release of powder from device while optimum aerodynamic property including FPF and MMAD ensure the sufficient lung deposition and local targeting of dried powders with improved stability of NPs**.**

6.3.6. *In-vitro* release kinetics

Unlike fast and 100% CIPR release from pure ciprofloxacin dispersion within 6 h, CIPR-CH-NPs exhibited initial burst release up to 44.1±4.3% in first 3 h followed by sustained release up to 89.3±5.3% in 24 h (Figure 6.7). Further, the model fitting demonstrated diffusion controlled drug release with maximum regression coefficient in the Higuchi equation (r^2, 0.945).

The above findings can be explained based on the following fact. Apart from the dispersion of the drug in the polymeric matrix, the hydrophilic drug also achieves NPs surface deposition offering to initial burst release, followed by sustained release up to 24 h (Enayati, Stride et al. 2012). The above discussion supports the *in-vitro* release of NPs displayed in Figure 6.7 in this study. The biphasic release profile deliver advantage over conventional therapy (Cheow, Chang et al. 2010) by preventing the development

of antibiotic tolerance for microbes and the similar effect was reflected in MIC and MBIC observations.

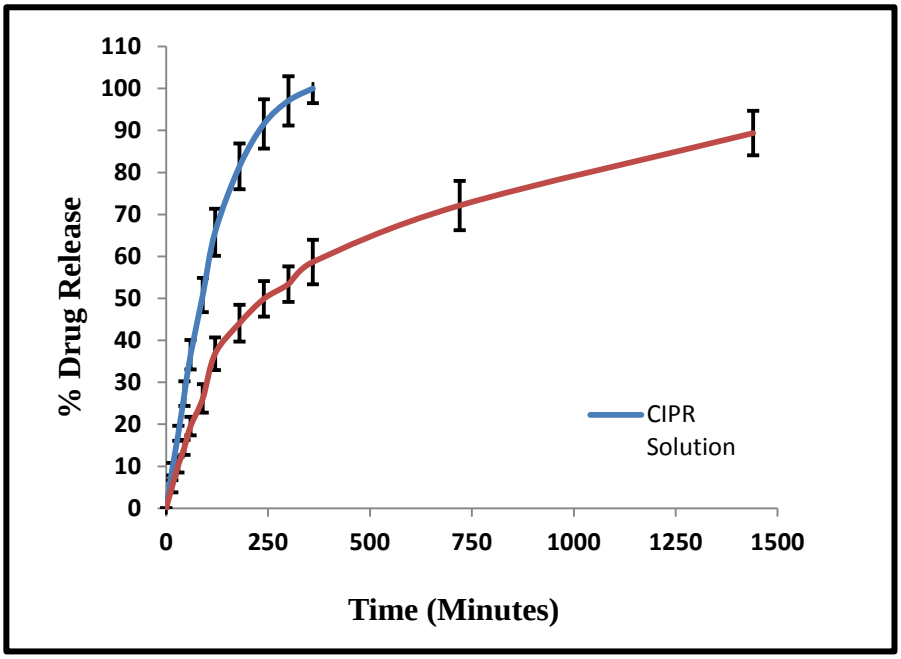

Figure 6.7: Comparative *in-vitro* release profile of CIPR-CH-NPs and CIPR.

6.3.7. FTIR spectra

As shown in Figure 6.9, FTIR spectra of pure CIPR exhibited intense transmittance peaks for stretching vibration at wave number 3520.02, 3374.6, 3077.9 - 2929.5, 1706.8 and 1607.4 cm^{-1}explicitly representing the presence of O-H group, N-H group at piperazinyl ring, aliphatic/aromatic C-H, carboxyl group (C=O) and C=O group at quinolone ring respectively, in CIPR structure. Moreover, all the above peaks conforming to CIPR were also visible in the FTIR spectra of physical mixture and CIPR-CH-NPs confirming the compatibility of CIPR with CH. The analysis of FTIR spectra illustrated in Figure 6.9 suggested that the significant interaction which can lead to loss of drug activity or toxicity was absent, as all the IR peaks conforming to CIPR functional group were intact in CIPR-CH-NPs spectra.

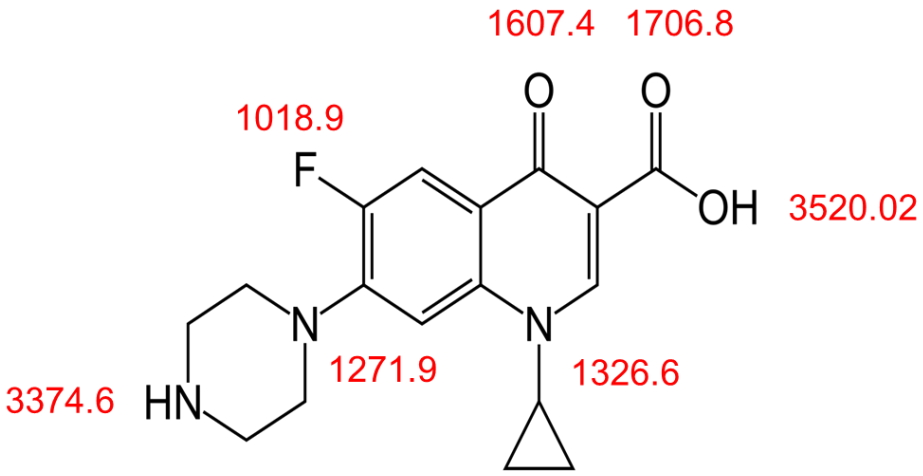

Figure 6.8: Schematic representation of FTIR peaks on the ciprofloxacin structure.

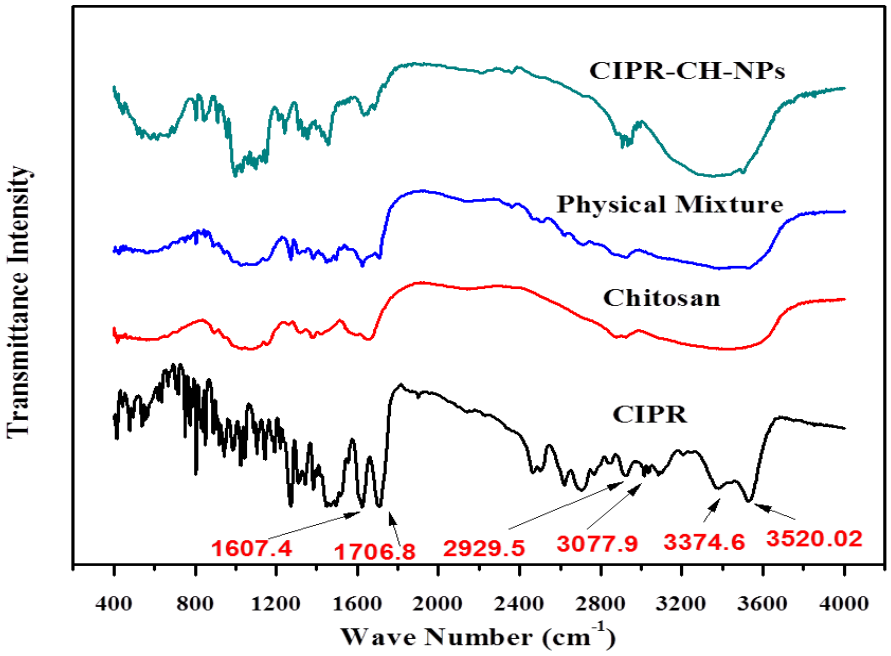

Figure 6.9: FTIR spectra of the different test samples.

6.3.8. XRD spectra

Diffraction pattern in Figure 6.10 for CIPR with the intense peak at 2θ 11.7, 13.9, 15.2, 19.4, 20.9, 23.15, 24.92, 26.45, 29.08, 20.4, 35.68, 39.2, 41.8, and 47.12^{o} signified that CIPR was in the crystalline state. However, the diffraction intensity of the CIPR-CH-NPs was lost or reduced significantly. Findings of XRD study showed that, though pure CIPR had the crystalline structure with the number of sharp and intense peak in the diffraction pattern, the diffraction peaks after fabrication of CIPR-CH-NPs either lost or replaced with the plateau. The loss of diffraction peaks in XRD spectra of CIPR-CH-NPs suggested that encapsulation of CIPR in chitosan nanoparticles resulted in amorphization or dispersion in molecular form in the chitosan matrix during the NPs formation.

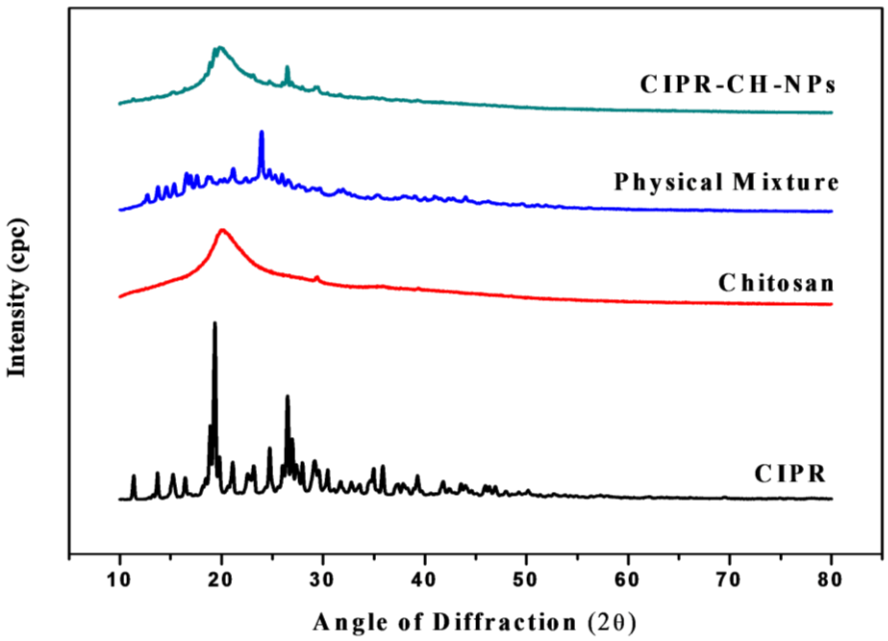

Figure 6.10: XRD diffraction pattern of the different formulation.

6.3.9. Minimum Inhibitory Concentration

The MIC of CIPR and different nanoparticles tested *in-vitro* against the planktonic mucoid *P. aeruginosa* is shown in Table 6.3. The MIC of pure CIPR, CIPR+AgLase

and other nanoparticles (CIPR-CH-NPs, CIPR-CH-NPs+AgLase and AgLase-CIPR-CH-NPs) after 24 h was 0.0625 and 0.125 µg/mL, respectively. After 48 h the MIC of pure CIPR and CIPR+AgLase shifted to 0.125 µg/mL while MIC value of CIPR-CH-NPs and AgLase-CIPR-CH-NPs was unaltered and did not show the sign of bacterial growth. The results of MIC for chitosan, CH-NPs and AgLase-CH-NPs without CIPR against *P. aeruginosa* was also observed in similar fashion and had 1.25, 0.937 and 0.937 mg/mL MIC, respectively. While the pure AgLase did not possesses any antimicrobial effect on given concentrations. The observed findings with improved antimicrobial activity of NPs may be attributed to higher penetration and microbial cell adhesion.

Furthermore, the findings of MIC assay were convincing as CIPR-CH-NPs, and AgLase-CIPR-CH-NPs demonstrated prolonged inhibition of microbial growth on single dose till 48 h, while the CIPR solution could not maintain its activity beyond 24 h and the MIC was increased with extensive sign of microbial growth. The improved antimicrobial activity can be explained either by higher penetrability, and microbial cell adhesion by biphasic release of NPs in which burst release and sustained release offers the loading and maintenance dose of CIPR, respectively, to maintains antimicrobial activity for longer duration (Wang, Hu et al. 2017).

6.3.10. Minimum Biofilm Inhibitory concentration (MBIC)

MBIC is a concentration at which formulation prevents the adherence of biofilm in planktonic bacterial suspension on incubation. Therefore, an *in-vitro* study against planktonic *P. aeruginosa* was conducted to determine the biofilm inhibition potential of NPs. Though CIPR+AgLase and CIPR-CH-NPs+AgLase produced slightly higher

inhibition than CIPR and CIPR-CH-NPs alone, they all completely restrained the biofilm at same 0.25 µg/mL concentration of CIPR (Figure 6.11).

Table 6.3: MIC and MBEC of different formulations

S. no.	Formulation	MIC (µg/mL; mg/mL*)	
		24 h	48 h
1	Pure CIPR	0.0625	0.125
2	CIPR+ AgLase	0.0625	0.125
3	CIPR-CH-NPs	0.125	0.125
4	CIPR-CH-NPs+AgLase	0.125	0.125
5	AgLase-CIPR–CH-NPs	0.125	0.125
6	Chitosan	1.25*	2.50*
7	Placebo CH-NPs	0.983*	1.25*
	Placebo AgLase-CH-NPs	0.983*	1.25*

Footnote: CIPR stands for ciprofloxacin; AgLase denotes Alginate Lyase; CIPR+AgLase represent the mixture of ciprofloxacin and Alginate Lyase; CIPR-CH-NPs signifies ciprofloxacin loaded chitosan Nanoparticles; AgLase-CIPR-CH-NPs symbolizes AgLase Functionalized chitosan Nanoparticles of Ciprofloxacin.

Unlike the 24 h, after 48 h (Figure 6.12) pure CIPR and CIPR+AgLase displayed the significant increase in the biofilm formation (for pure CIPR 4.6±1.4% to 6.3±1.2% at 0.0625 µg/mL) and even exhibited biofilm formation on 0.25 µg/mL concentration. Whereas, CIPR-CH-NPs, CIPR-CH-NPs+AgLase, and AgLase-CIPR-CH-NPs did not show any tolerance and were equally effective as the day first in restraining the biofilm, where, AgLase-CIPR-CH-NPs alone showed lowest 2.5+1.2% and 2.8+1.2% biofilm formation at 0.0625 µg/mL after 24 and 48 h, respectively.

Though pure CIPR and NPs equivalently inhibited the biofilm formation after 24 h in MBIC study, NPs were excellent in producing the biofilm inhibitory effect and

maintained it for 48 h as compared to pure CIPR. It can be explained based on the higher efficiency of NPs to penetrate mucin and prevent the steric resistance, higher cell adhesion (Al-Nemrawi, Alshraiedeh et al. 2018) and sustained drug release in close proximity of bacteria which may have avoided the development of microbial tolerance (Cheow, Chang et al. 2010), and also due to AgLase which is supposed to hydrolyze the alginate produced by mucoid *P. aeruginosa at* glycosidic linkage and prevent the microbial adherence to surface (Hatch and Schiller 1998, Alkawash, Soothill et al. 2006). The similar results after 24 h were observed in the previous study on biofilm inhibition showing the efficacy of DNase-I functionalized NPs against *P. aeruginosa* (Baelo, Levato et al. 2015).

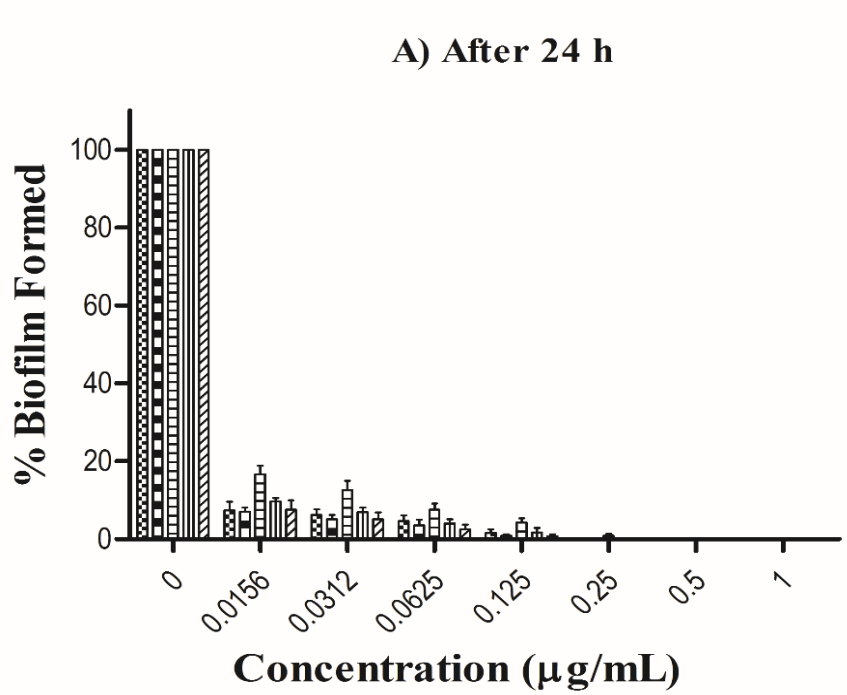

Figure 6.11: The comparative findings of the MBIC after 24 h treatment.

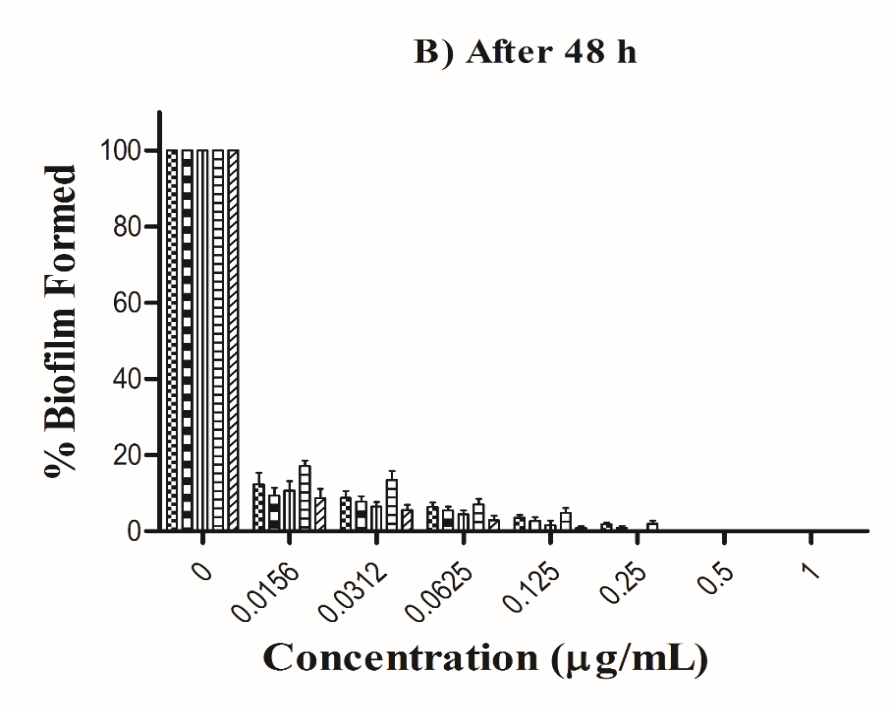

Figure 6.12: The comparative findings of the MBIC after 48 h treatment.

6.3.11. Minimum Biofilm Eradication Concentration (MBEC)

It is apparent from the MBEC values of different formulations given in Table 6.4 that AgLase-CIPR-CH-NPs demonstrated the most promising results against the 48 h grown *P. aeruginosa* biofilm and completely shrank it at 0.5 µg/mL concentration, whereas, the MBEC for pure CIPR, CIPR+AgLase, CIPR-CH-NPs, CIPR-CH-NPs+AgLase was found to be 3, 2, 2, and 1 µg/mL, respectively. Although each group produced higher biofilm dispersal on increasing the concentration, AgLase-CIPR-CH-NPs alone have shown highest biofilm dispersal potential as compared to others and inhibited around 97% of biofilm at 0.25 µg/mL after 24 h. Similarly, CIPR-CH-NPs also exerted higher anti-biofilm activity compared to the pure CIPR and equivalent to CIPR+AgLase which may be due to increased mobility or penetration of the NPS in the matrix pores. Interestingly, MBEC of pure CIPR, CIPR+AgLase, was quite high (Table 6.4) as compared to AgLase-CIPR-CH-NPs, apparently due to comparatively low penetration

and mobility of CIPR alone in biofilm matrix which imposes high tolerance to the antibiotic therapy (Tré-Hardy, Vanderbist et al. 2008, Van Acker, Van Dijck et al. 2014). On contrary, AgLase improves the penetration, mobility and distribution of drug and NPs in the biofilm matrix by hydrolyzing the alginate (Baelo, Levato et al. 2015), and therefore, NPs attained the higher concentration of drug nearby bacterial colonies embedded in biofilm and thus enhanced the antibiotics susceptibility (Jørgensen, Wassermann et al. 2013, Nafee, Husari et al. 2014). Although CIPR+AgLase and CIPR-CH-NPs+AgLase demonstrated significantly higher antibiofilm activity against *P. aeruginosa* biofilm, yet AgLase-CIPR-CH-NPs alone rendered the highest biofilm depletion even at the lowest concentration.

At the same time, results of repeated dosing (0.125 µg/mL) shown in Figure 6.13 demonstrated that unlike pure CIPR, CIPR+AgLase, CIPR-CH-NPs, and CIPR-CH-NPs+AgLase, AgLase-CIPR-CH-NPs entirely dissembled the extracellular matrix of biofilm and reduced the microbial load completely after three successive dosing (72 h). Moreover, chitosan, CH-NPs and AgLase-CH-NPs without CIPR exhibited antimicrobial activity though, but failed to completely remove bioburden from the biofilm even at highest concentration and hence getting the MBEC values could not be possible.

Table 6.4: Minimum biofilm eradication concentration of the various formulations.

S. no.	Formulation	MBEC (µg/mL)
1	Pure CIPR	3
2	CIPR+ AgLase	2
3	CIPR-CH-NPs	2
4	CIPR-CH-NPs+AgLase	1
5	AgLase-CIPR–CH-NPs	0.5

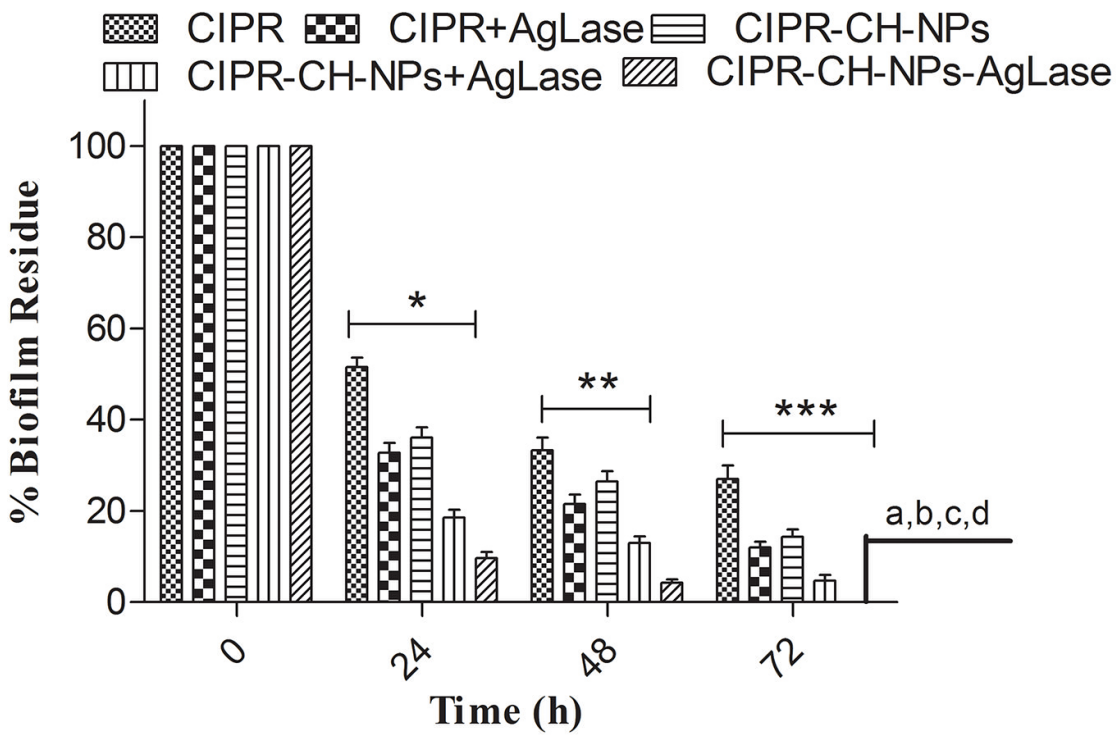

Figure 6.13: Antimicrobial studies. A and B represents the MBIC after 24 and 48 h. The microbial count in control group was 1.8 x 10^8± 9.8 x 10^6 CFU/mL after 24 h and 2.9 x 10^9± 1.9 x 10^8 CFU/mL after 48 h. Moreover, C and D illustrated the results of MBEC study showing reduction of 48 h grown *P. aeruginosa* biofilm on single dose at different CIPR concentrations and on repeated dosing of formulations (0.125 µg/mL) for three consecutive days respectively. Two-way ANOVA was performed (where * represents $p<0.05$; other groups vs AgLase-CIPR-CH-NPs). The viable count in the controlled experiments without any treatment was 2.45 x 10^9 ± 1.23 x 10^8 CFU/mL.

6.3.12. Microscopic study of biofilm

CLSM was performed to further confirm the antibiofilm potential of AgLase functionalized NPs on *P. aeruginosa* biofilm grown for 48 h on the glass coverslip in 12 well plate. The data depicted in Table 6.5 regarding biomass and thickness was determined from z stack CLSM images (Figure 6.14A-6.14F) using COMSTAT 2 software. Biofilm without treatment served as control and exhibited highest biomass and thickness (61.5±3.16 µm). Though, all the formulations had negative effect on

biofilm and reduced its biomass and thickness on treatment, AgLase-CIPR-CH-NPs convincingly demonstrated highest antibiofilm activity with lowest biomass 9.1±1.3 $\mu m^3/\mu m^2$ and thickness (14.2±2.03 µm) of biofilm.

All these findings supported the hypothesis produced in this research and illustrated that AgLase functionalized chitosan NPs of CIPR had significantly improved the antibacterial and anti-biofilm potential by disrupting the extracellular matrix in biofilm and killing the protected microbial colonies.

Table 6.5: Thickness and Biomass of biofilm treated with different formulation

	Biofilm Parameters (Mean±SD)	
Treatment	**Thickness (µm)**	**Biomass ($\mu m^3/\mu m^2$)**
Control (untreated)	61.5±3.16	36.2±4.1
CIPR	50.7±4.05	27.5±2.9
CIPR+AgLase	40.6±2.03	23.9±3.1
CIPR-CH-NPs	34.5±2.02	24.5±2.6
CIPR-CH-NPs+AgLase	21.6±1.17	17.8±1.5
AgLase-CIPR-CH-NPs	14.2±2.03*	9.1±1.3*

*represents the significant difference in thickness and Biomass of biofilm treated with different formulation compared to AgLase-CIPR-CH-NPs ($p<0.05$; One-way ANOVA); Values represents mean of 3 replicates with standard deviation (Mean±SD).

6.3.13. MTT assay

The findings of MTT assay for lungs epithelium cell line after 24 h treatment with different formulations are depicted in Figure 6.15. The results of MTT assay assured the well-tolerated cytocompatibility of NPs on human lung epithelium cell line. NPs appeared to have very low cytotoxicity at all the tested concentrations of CIPR.

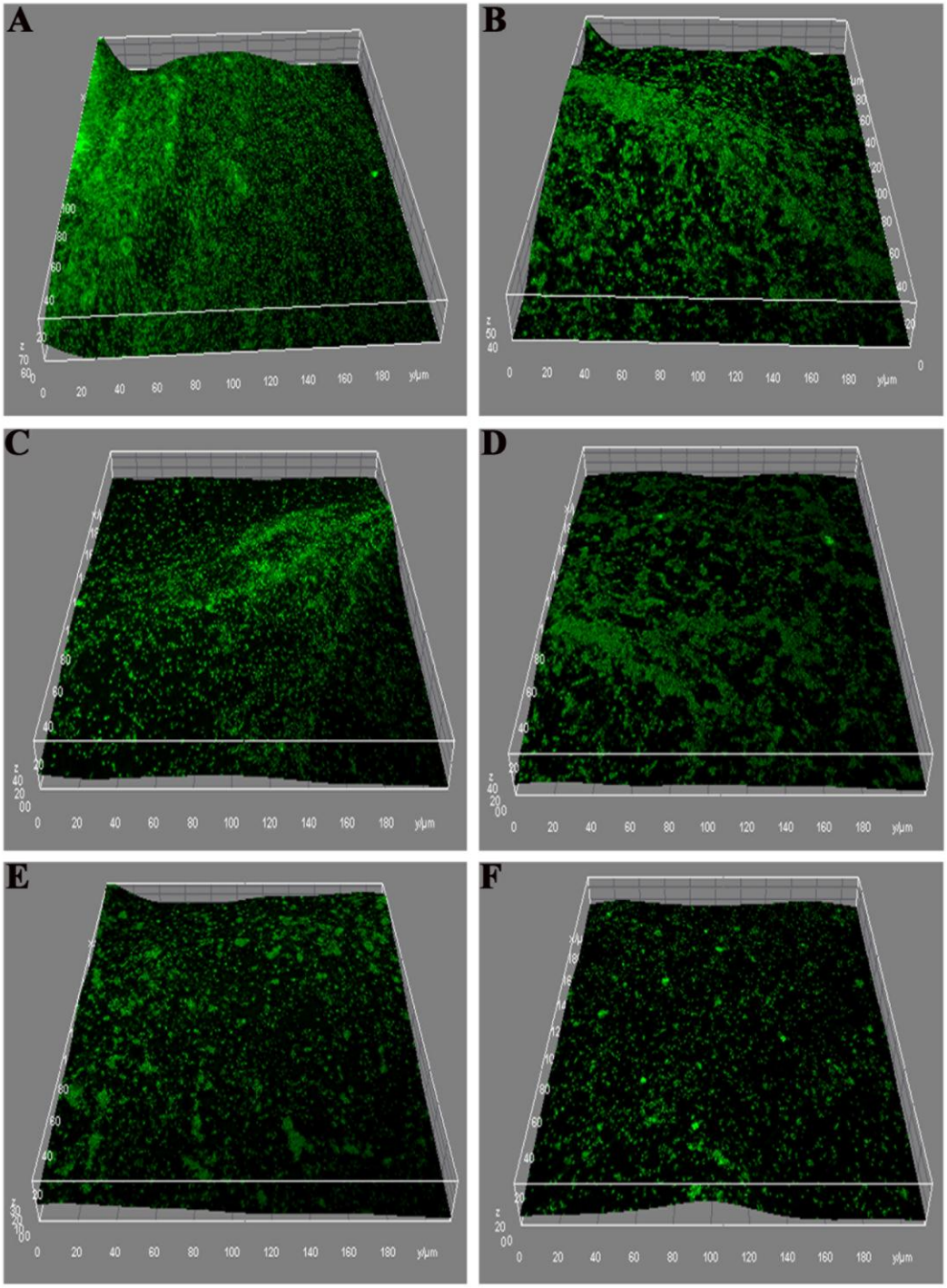

Figure 6.14: CLSM images of biofilm showing the relative density of biofilm. Where A, B, C, D, E and F denote Control or untreated, CIPR, CIPR+AgLase, CIPR-CH-NPs, CIPR-CH-NPs+AgLase and AgLase-CIPR-CH-NPs treated biofilm of *P. aeruginosa,* respectively.

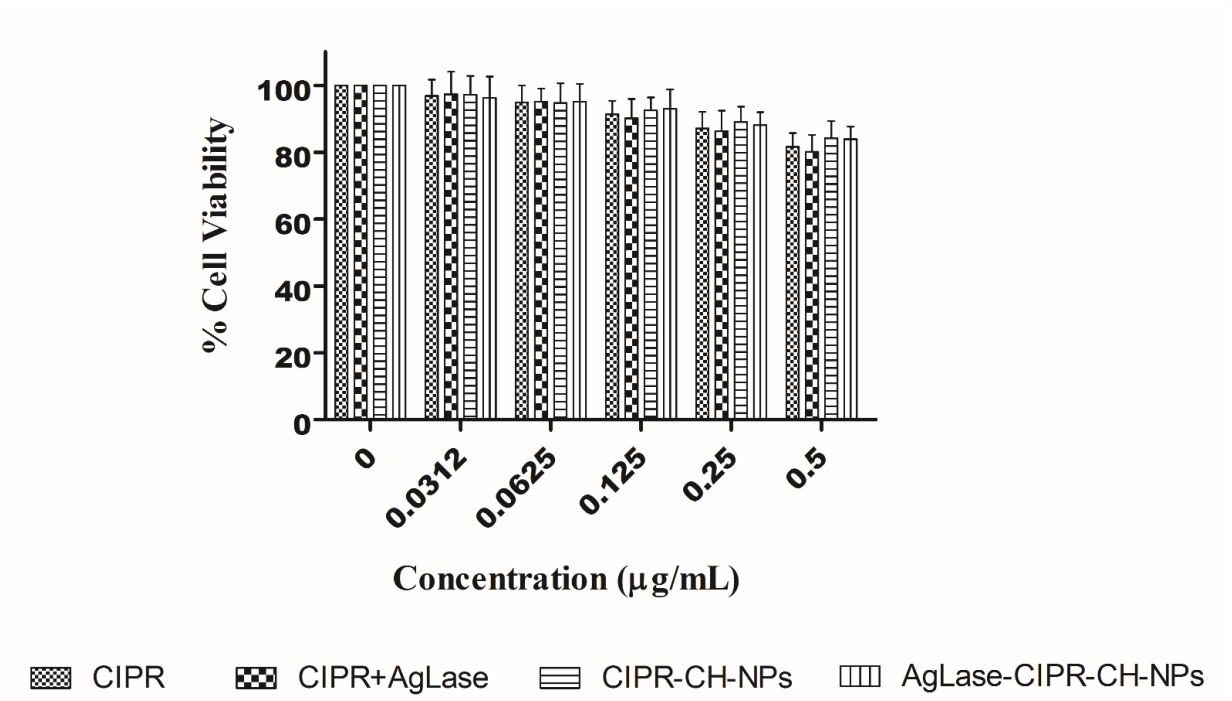

Figure 6.15: Bar graph elaborates the findings of the in-vitro cytotoxicity study

6.3.14. Haemolysis

Lungs are highly vascularized organ responsible for gases exchange between alveoli and pulmonary blood vessels consequently pulmonary administration of NPs may lead to direct interaction with blood component. Therefore, we performed haemocompatibility study. International standards recommend that any formulation supposed to have direct exposure to the blood or blood vessels should not possess more than 1% haemolytic potential (Vijayakumar, Kumari et al. 2016).

As depicted in Figure 6.16, all the test samples including CIPR, AgLase, CIPR-CH-NPs and AgLase-CIPR-CH-NPs exhibited almost similar haemolytic profile. None of the formulation showed more than 1% haemolysis even at highest concentration 0.25 µg/mL equivalents to CIPR and 100 µg/mL equivalent to AgLase, % indicative of the potential safety of the developed formulation for pulmonary delivery.

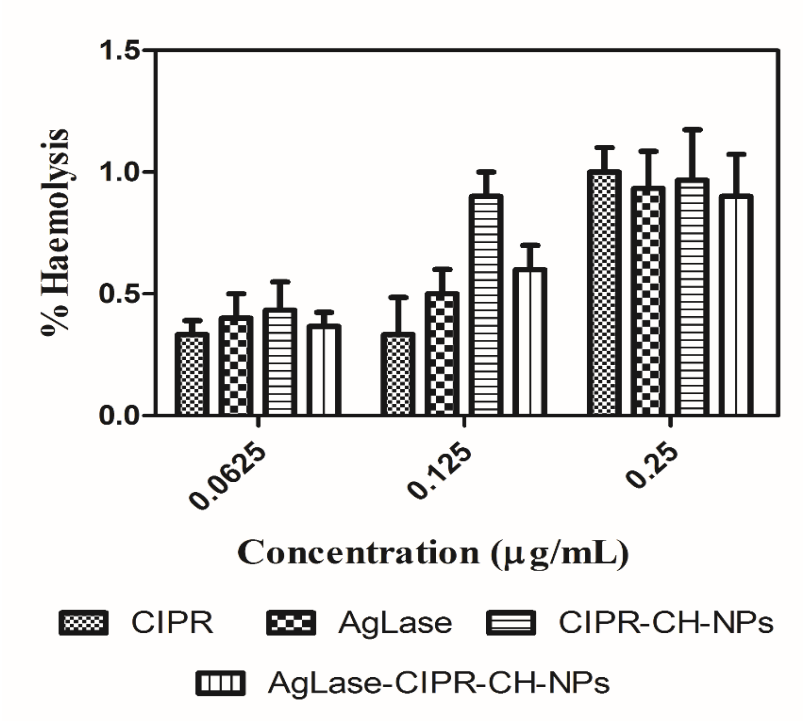

Figure 6.16: Percent haemolysis after incubating the processed blood sample with formulations.

6.3.15. Platelet aggregation

Similar to the haemolysis, excessive platelet aggregation in the blood vessels may lead to vascular or cardiac disorders including transient ischaemia, myocardial infarction or stroke (Vijayakumar, Kumari et al. 2016). Thus, formulation to be administered through intravenous route or may have direct contact with blood must be tested for platelet aggregation potential. The result shown in Figure 6.17 clearly indicated that CIPR and AgLase did not show significant change in the platelet count after 8 h treatment. However, the CIPR-CH-NPs and AgLase-CIPR-CH-NPs exhibited slightly lower but insignificant count on treatment and could be attributed to the haemostatic nature of chitosan (Chou, Fu et al. 2003). Any possible toxicity due to the formulation component was further ruled out by qualitative analysis of platelet aggregation (Figure 6.18a–6.18o).

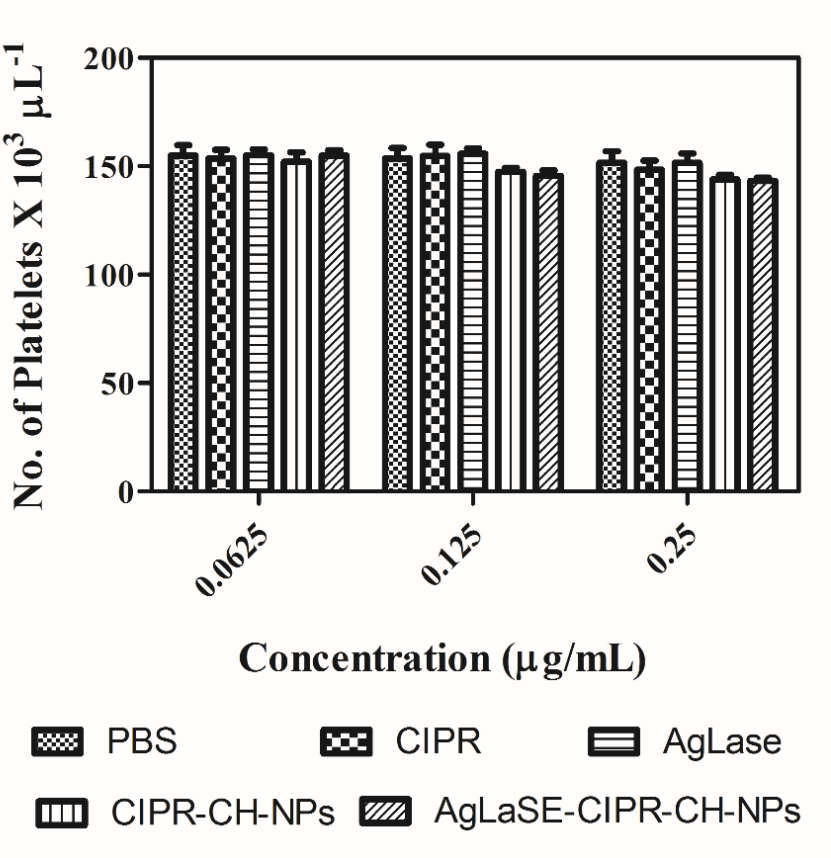

Figure 6.17: Platelet count in blood after treatment with different formulation at different concentration (0.0625, 0.125 and 0.25 µg/mL).

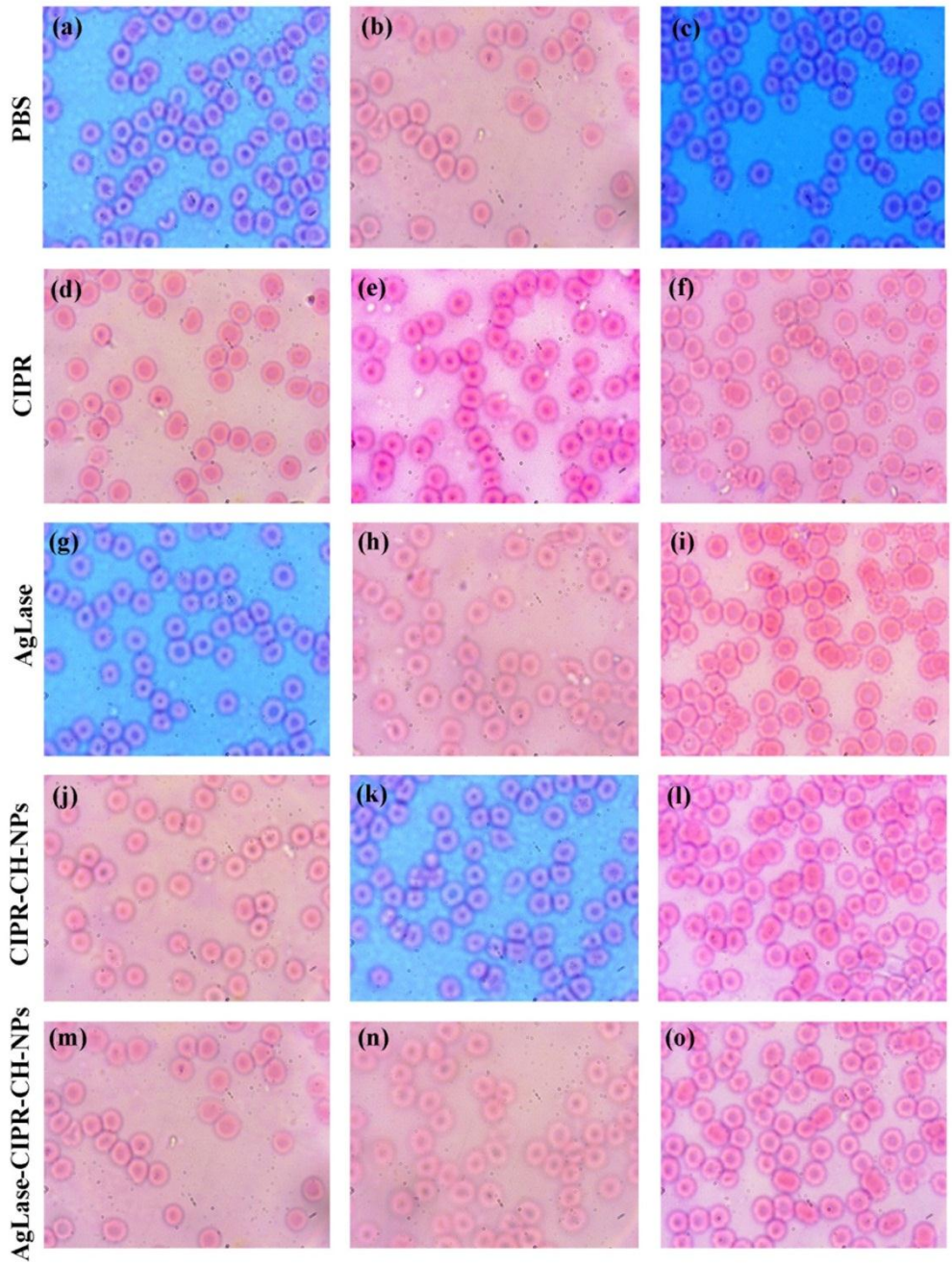

Figure 6.18: Leishman's stained microscopic images of whole blood samples after treating with PBS equivalent to 0.0625, 0.125, and 0.25 µg/mL of test sample (a, b and c resp.); CIPR at 0.0625, 0.125, and 0.25 µg/mL concentration (d, e and f resp.); AgLase at 10, 50 and 100 µg/mL concentration (g, h and I resp.); CIPR-CH-NPs equivalent to 0.0625, 0.125, and 0.25 µg/mL CIPR concentration (j, k and l resp.) and: AgLase-CIPR-CH-NPs equivalent to 0.0625, 0.125, and 0.25 µg/mL CIPR concentration (m, n and o resp.).

6.3.16. *In vivo* toxicity study

Furthermore, the toxicity of the developed formulation was tested *in-vivo* against lung epithelia as prolonged exposure of formulation may cause disruption of lung epithelia. Lungs possess its unique microenvironment essential for the gases exchange and lungs surfactant play crucial role in maintaining the pulmonary function normal. Therefore, *in-vivo* lungs toxicity study was performed to evaluate the morphological change in lungs. The HE stained histological image of animal lungs treated with CIPR (Figure 6.19b), AgLase (Figure 6.19c), CIPR-CH-NPs (Figure 6.19d) and AgLase-CIPR-CH-NPs (Figure 6.19e) did not show any sign of tissue toxicity indicating the safety and tissue compatibility of the developed NPs.

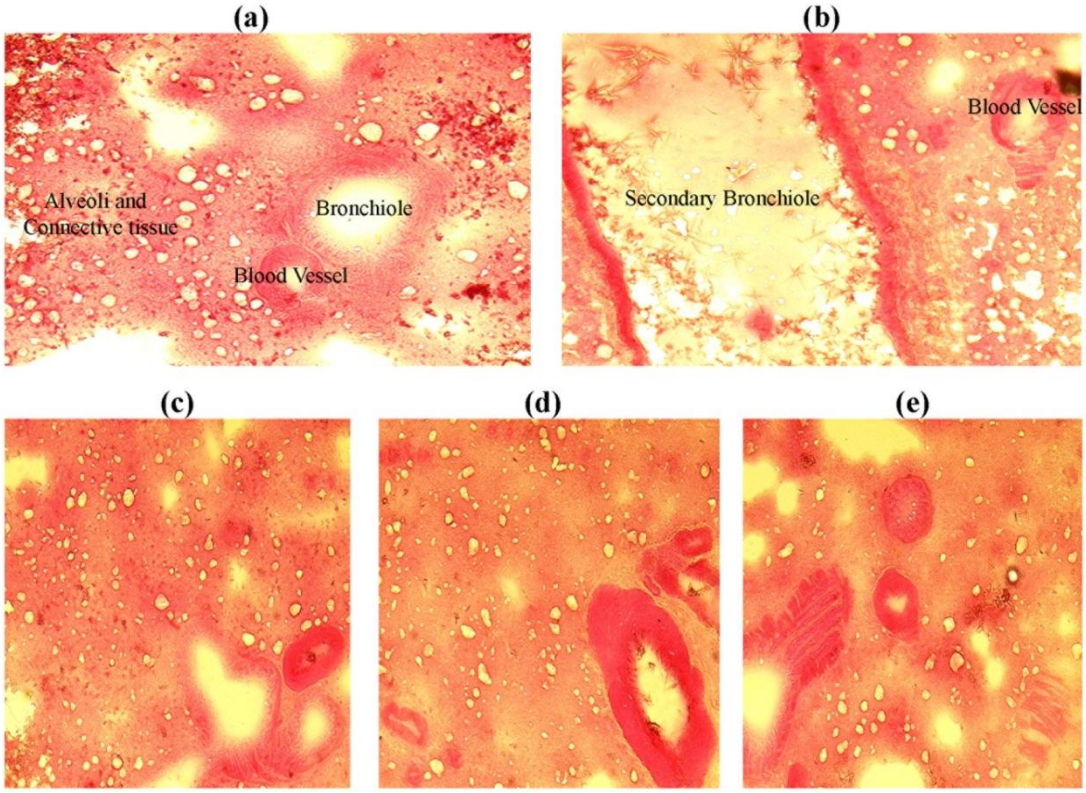

Figure 6.19: HE stained histological images of animal lungs treated for 7 consecutive days with different formulations. a) Untreated; b) CIPR treated; c) AgLase treated; d) CIPR-CH-NPs treated and; e) AgLase-CIPR-CH-NPs treated.